Gene expression profile analysis on different stages of hypertrophic scarring in a rabbit ear model

JI ZHU*, MENGYAN SUN*, YUCHONG WANG*, HONGDA BI and CHUNYU XUE

Department of Plastic Surgery, Changhai Hospital, Second Military Medical University, Shanghai 200433, P.R. China

Received October 30, 2018; Accepted December 4, 2019

DOI: 10.3892/etm.2020.8879

Abstract. Hypertrophic scarring (HS) is one of the most common skin disorders. The study aimed to investigate the gene expression profile at day 10 (Stage 1), 21 (Stage 2), and day 40 (Stage 3) post-wounding of HS using RNA-sequencing of a scar model from rabbit ears. A total of 17,386 unigenes were annotated using the eggNOG Functional Category database. The study identified significantly differentially expressed genes (DEGs) including 261, 141, and 247 upregulated ones as well as 253, 272, and 58 downregulated ones in three stages respectively. The DEGs varies among each stage measured by Gene Ontology (GO) terms and Kyoto Encyclopedia of Genes and Genomes (KEGG) pathways. DEGs were enriched in 'immune system process' and 'proteinaceous extracellular matrix' in Stage 1, 'anatomical structure development', 'cell differentiation', 'cell adhesion'and some other terms in Stage 2, 'cancers', 'proteinaceous extracellular matrix' and 'signal transduction' in Stage 3. Furthermore, the Wnt signaling pathway was found to play a pivotal role in regression of HS. In conclusion, we revealed comprehensively the gene expression profiles during HS formation providing probable targets in HS treatment.

Introduction

Wound healing and scarring can be divided into three stages: Inflammation, proliferation and tissue remodeling; these are complex processes, involving a variety of cell types, cytokines and signaling pathways (1). Hypertrophic scarring (HS) is a manifestation of a dysfunctional response to dermal injury and is characterized by excessive deposition of the extracellular matrix and excessive proliferation of fibroblasts (2). HS is one of the most frequent skin diseases, mainly occurring in 30-72% of patients with thermal injury and trauma (3). HS can cause cosmetic disfiguring or produce restriction of motion (1). Growth factors, such as transforming growth factor-β (4), cytokines [including interleukin (IL)-4, 8 and 10, and interferon-γ (5,6)], chemokines [including stromal cell-derived factor-1 (7), CXC chemokine receptor 3 (CXCR3) (8) and monocyte chemotactic protein-1 (9)] and proteolytic enzymes [including matrix metalloproteinase (MMP)-1, 2 and 9 (10,11)] have been suggested to be involved in the molecular mechanism of the pathogenesis of HS. However, due to the complexity of HS, a complete understanding of the molecular mechanism underlying the formation of HS has not yet been elucidated.

High throughput RNA-sequencing (RNA-Seq) using next-generation sequencing technology enabled effective and comprehensive analysis of the gene expression profile in previous studies (12-14). In the present study, an animal model of HS was established using a rabbit ear (6,15), and then the general pattern of the gene expression profile in HS and control samples was investigated during different stages using RNA-Seq. The differentially expressed genes (DEGs) and biological pathway alterations were identified. The present study may provide a better understanding of the molecular mechanisms involved in the formation of HS.

Materials and methods

Hypertrophic scar model and sample collection. All animal experiments were approved by The Institutional Animal Care and Use Committee of The Second Military Medical University. Hypertrophic scars were created in 50 one-year old female New Zealand White rabbits (Shanghai SLRC Experimental Animal Co., Ltd.) (6). Rabbits weighed 2.5 kg at the beginning of the experiment. Each rabbit was raised in separate cages at 25˚C with constant laminar flow and circadian light/dark cycle (light, 6 am-4 pm; dark 4 pm-6 am). Rabbits had access to food and water 4-5 times a day. The rabbits were anesthetized with 30 mg/kg sodium pentobarbital. A total of four full-thickness wounds (1.5x1.5 cm) were created down to the bare cartilage on the ventral surface of each ear, in which the incision interval was >1.5 cm. After bleeding was stopped by applying pressure, the ventral surface of the ear was bandaged with dressing. Scar formation was checked daily. The stages of

Correspondence to: Dr Chunyu Xue, Department of Plastic Surgery, Changhai Hospital, Second Military Medical University, 168 Changhai Road, Yangpu, Shanghai 200433, P.R. China
E-mail: xcyfun@126.com

*Contributed equally

Key words: Gene Ontology, Kyoto Encyclopedia of Genes and Genomes, hypertrophic scar, RNA-sequencing, Wnt signaling pathway

wounding were divided according to the average time of peak inflammation (Stage 1), peak scar hypertrophy (Stage 2) and complete degraded appearance of scarring (Stage 3) (6). At 10 (Stage 1), 21 (Stage 2) and 40 (Stage 3) days post-wounding the rabbits were sacrificed, and hypertrophic scarring (HS; 1HS, 2HS and 3HS) tissues and corresponding control (C) samples (1C, 2C and 3C) were collected, snap frozen in liquid nitrogen and stored at -80˚C (Fig. 3A). The surrounding scars are as control (C) samples (1C, 2C, 3C).

Hematoxylin & eosin (H&E) staining and Masson's trichrome staining. H&E staining was performed as previously described (16). Tissue samples with mean border thickness of 1.9 mm were stored overnight in 10% formalin at room temperature, dehydrated in ethanol, cleared in xylene and paraffin embedded. Cross-sections (6 μm) were prepared for staining with H&E and Masson's trichrome for histological evaluation. Masson's trichrome staining was applied to examine collagen deposition with a light microscope at x40 and x100 objective (Olympus).

RNA isolation. Total RNA was extracted using TRIzol® reagent (Invitrogen; Thermo Fisher Scientific, Inc.) according to the manufacturer's instructions. The isolated RNA was then treated with DNase I (Thermo Fisher Scientific, Inc.) to remove the genomic DNA. The quantity and quality of the RNA were assessed using Agilent 2100 Bioanalyzer (Agilent Technologies, Inc.).

cDNA library construction, sequencing, data filtering and alignment. In the present study, mRNA was enriched from total RNA with magnetic beads with oligo-dT, and then mixed with 10X fragmentation buffer (Enzymatics) to obtain short fragments of 200-300 nt. First-strand cDNA was synthesized from the fragments with random hexamer primers, and then transformed into double-strand cDNA using RNase H and DNA polymerase I (Takara Bio, Inc.). Fragments of desirable lengths (200-300 bp) were purified using the QIAquick PCR Extraction kit (Qiagen) and linked with sequencing adaptors after end repair. Once inappropriate fragments were removed using AMPure XP beads (Beckman Coulter, Inc.), the sequencing library was constructed using PCR. The following thermocycling conditions were used for the PCR: U-chain degradation at 37˚C for 10 min; Initial denaturation at 98˚C for 30 sec; 12 cycles of 98˚C for 10 sec, 60˚C for 30 sec, 72˚C for 30 sec; and a final extension step of 72˚C for 5 min. DNA fragments with ligated adaptor molecules on both ends were selectively enriched using Illumina PCR Primer Cocktail (Illumina, Inc.) in a 12-cycle PCR reaction. The quantity, length and the distribution of the fragments in the cDNA libraries were checked using PicoGreen (Quantifluor™-ST fluorometer E6090; Promega Corporation) and a fluorospectrometer (Quant-iT PicoGreen dsDNA Assay kit; Invitrogen; Thermo Fisher Scientific, Inc.), and then quantified with Agilent 2100 Bioanalyzer.

The libraries were diluted to 4-5 pM and sequenced using the Illumina NextSeq™ 500 platform (Illumina, Inc.). The raw reads were filtered by removing the adapter sequences and the low-quality sequences (length <50 bp or Q score <20). RNA-Seq data were aligned to the rabbit genome (Oryctolagus_cuniculus.OryCun2.0.dna.toplevel.fa) using Bowtie 2 (http://tophat.cbcb.umd.edu/).

Gene functional annotation and classification. The gene annotation was obtained from ENSEMBL (http://ensemblgenomes.org/). The genes were also annotated with the eggNOG database (http://www.ncbi.nlm.nih.gov/COG/; http://eggnog.embl.de/version_3.0/). DEGs with 2-fold up- or down-regulation with a P-value <0.05, were identified using HTSeq (http://www-huber.embl.de/users/anders/HTSeq) followed by DESeq (http://www-huber.embl.de/users/anders/DESeq). The volcano plot was used to visualize DEGs. For a further functional understanding of the DEGs, Gene Ontology (GO) (http://www.geneontology.org/) annotations were determined based on the GOSlim database (http://www.geneontology.org/). The Kyoto Encyclopedia of Genes and Genomes (KEGG) database (version 90.1; http://www.genome.jp/kegg/) was utilized to achieve pathway annotations.

Reverse transcription-quantitative PCR (RT-qPCR). mRNA in the total RNA was reverse transcribed using a first strand cDNA synthesis kit (Toyobo Life Science) according to the manufacturer's protocol. RT-qPCR reactions were performed with SYBR Green Master Mix (Takara Bio, Inc.) on an Applied Biosystems 7300 detection system (Applied Biosystems; Thermo Fisher Scientific, Inc.). β-actin was utilized as an internal control. The sequences of the primers used in the study were obtained from https://pga.mgh.harvard.edu/primerbank/ and are shown in Data S3. The following thermocycling conditions were used for the PCR: Initial denaturation at 94˚C for 30 sec; 35 cycles of 94˚C for 10 sec, 60˚C for 10 sec, 72˚C for 10 sec; and a final extension step of 72˚C for 3 min. Expression levels of the different genes were analyzed using the $2^{-\Delta\Delta Cq}$ method (17).

Statistical analysis. The results from three experimental repeats were presented as the mean ± standard deviation. Differences between groups were analyzed with Student's t-test. P<0.05 was considered to indicate a statistically significant difference. Data were analyzed with SPSS 21.0 (IBM Corp.).

Results

Histological staining of scars. H&E staining and Masson's trichrome staining were performed on the tissues at different healing stages of the rabbit ear wounds. In Figs. 1 and 2 it was observed that the neovascularization and collagen synthesis at the inflammatory stage increased, compared with the area outside the wound in each corresponding sample, and inflammatory cells were scattered in infiltration. Collagen synthesis in the proliferative stage was increased and cell proliferation was observed as well. Collagen synthesis in the tissue remodeling stage was decreased, and the thickness of the epidermis in the latter two stages was thicker than that in the former (Figs. 1 and 2).

RNA-Seq and mapping. In order to better understand the transcriptomes of HS at different stages, high-throughput Illumina sequencing was performed for RNA samples extracted from the HS and C samples at 10 (1HS and 1C), 21 (2HS and 2C)

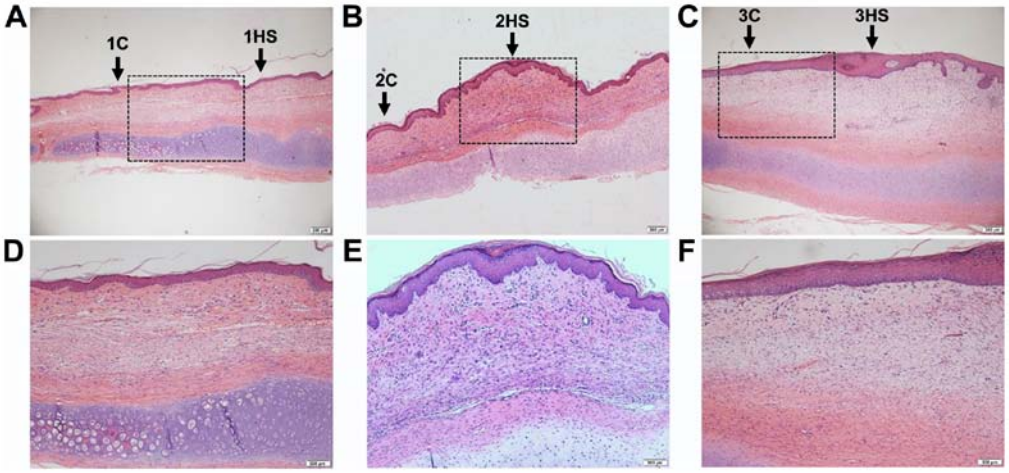

Figure 1. Hematoxylin and eosin staining of scars from rabbit ears at different stages. (A and D) Inflammatory stage; (B and E) proliferative stage; and (C and F) tissue remodeling period. The lower row (magnification, x100) is a higher magnification of the rectangular regions in the images above (magnification, x40). HS, hypertrophic scarring; C, control.

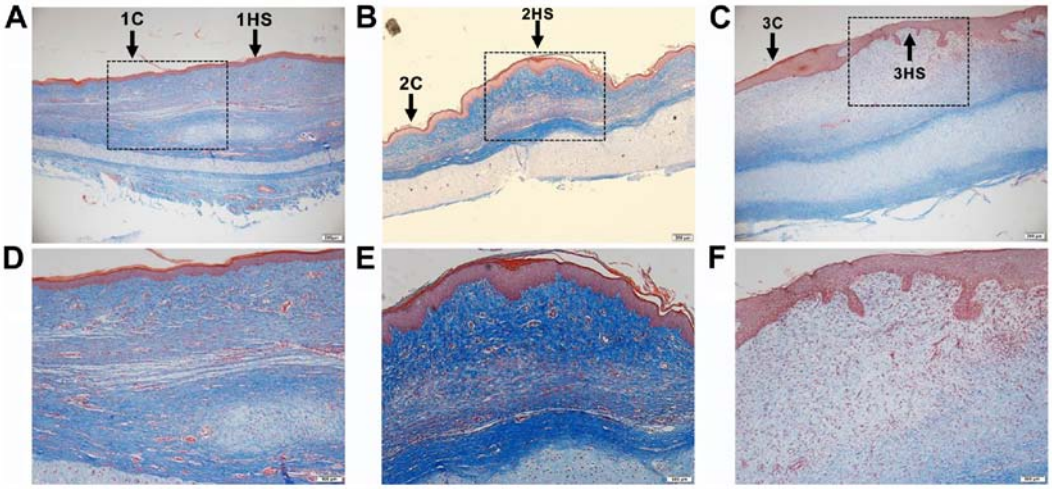

Figure 2. Masson's trichrome staining of scars from rabbit ears at different stages. (A and D) Inflammatory stage; (B and E) proliferative stage; and (C and F) tissue remodeling period. Collagen fibers and cartilage were stained blue, cytoplasm red, and nuclei blue black. The lower row (magnification, x100) is a higher magnification of the rectangular region in the images (magnification, x40). C, control; HS, hypertrophic scarring. HS, hypertrophic scarring; C, control.

and 40 (3HS and 3C) days post-wounding. The three stages are illustrated in Fig. 3A. From the RNA-Seq, a total of 223.4 million 150 bp paired-end raw reads were generated, with an average of 37.2 million reads per sample (Q20 >90% and Q30 >82%). After quality filtering, an average of 37.0 million clean reads per sample remained, with utilization of ~99% of the reads. After alignment to the rabbit genome, >70% mapped percentage was achieved and the majority of reads were mapped to unique positions (>94%; Table I).

Annotation and classification of unigenes. A total of 17,386 unigenes (73.5%) were annotated using the eggNOG Functional Category database (18). All of these unigenes were matched to 25 eukaryotic orthologous groups (Fig. 3B). The largest category was 'signal transduction mechanisms' (3,785; 20.99%). 'Function unknown' (2,663; 14.77%) and 'general function prediction only' (2,371; 13.15%) were the second and third largest categories, respectively.

Identification of DEGs. Genes that exhibited >2-fold differential expression with a P-value <0.05 were then defined as the DEGs. The hierarchical clusters separated DEGs according to their expression levels (Fig. 4A). The volcano plots showed the difference in expression levels of unigenes in HS and C tissues of each stage; the blue dots represent the number of DEGs (Fig. 4B-D). A total of 514, 413 and 305 DEGs were identified at days 10, 21 and 40 post-wounding, respectively Compared with the corresponding C group (1C, 2C and 3C), there were 261 upregulated DEGs at day 10, 141 at day 21 and 247 at day 40 post-wounding, as well as 253 downregulated DEGs at day 10, 272 at day 21 and 58 at day 40 post-wounding.

To validate data, DEGs at Stage 1 [IL8, C-C motif chemokine ligand 4 (CCL4) and dipeptidyl peptidase 4 (DPP4)], Stage 2 [MMP1, tenascin C (TNC) and transforming growth factor β-1 (TGFB1)] and at Stage 3 [Wnt family member 2B (WNT2B), insulin-like growth factor 2 mRNA-binding protein 1 (IGF2BP1) and versican (VCAN)] were randomly

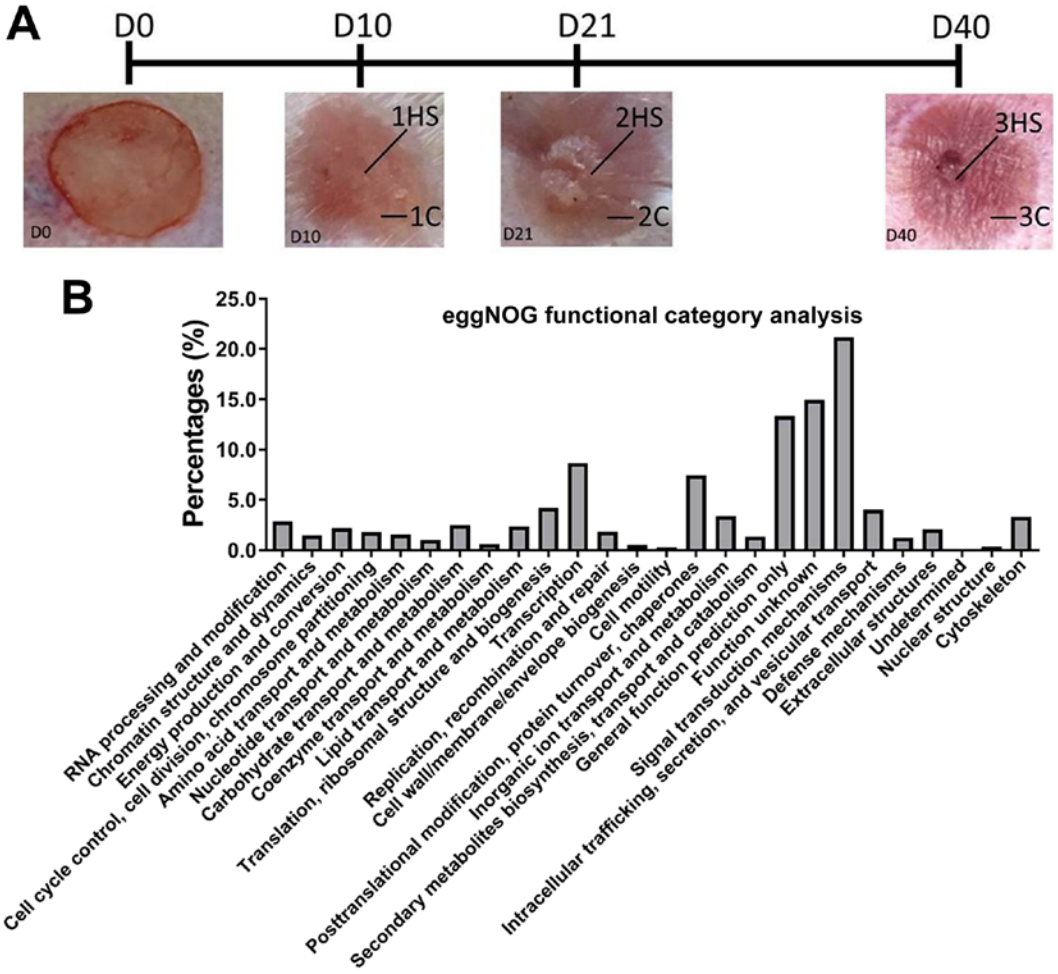

Figure 3. Global gene expression profile. (A) Times of different sampling. HS tissues (1HS, 2HS and 3HS) and corresponding C samples were obtained at D10, D21 and D40 post-wounding. (B) eggNOG annotation. HS, hypertrophic scarring; C, control; D, day.

picked for RT-qPCR analysis. As shown in Fig. 4E, nine significantly differentially expressed genes were randomly selected for validation experiments. Changes in the expression levels of detected genes by RT-qPCR were consistent with the results of RNA-Seq.

To further identify genes showing a significant change in expression level during different stages, Venn diagrams were constructed (Fig. 5). Only 6 and 8 DEGs were upregulated and downregulated in all three stages, respectively. The data suggested that the DEGs were varied during different stages.

Classification of DEGs. To determine the function terms in which DEGs were significantly enriched, GO function enrichment analysis was carried out. All DEGs were mapped into three main categories (molecular function, cellular component and biological process) in the GOSlim database. As illustrated in Figs. 6-8, 53 GO terms at 10 (Stage 1), 36 at 21 day (Stage 2), and 44 at 40 days post-wounding (Stage 3) were significantly enriched in DEGs ($P<0.05$). At Stage 1, 'extracellular region', 'immune system process' and 'proteinaceous extracellular matrix' were notably enriched in DEGs (Fig. 6A); at Stage 2, 'anatomical structure development', 'cell differentiation', 'locomotion', 'cell adhesion', 'cell proliferation', 'biological process' and 'cell motility' were markedly enriched in DEGs (Fig. 7A); at Stage 3, 'extracellular region', 'proteinaceous extracellular matrix' and 'extracellular space' were significantly enriched in DEGs (Fig. 8A).

KEGG pathway enrichment analysis was performed to identify the significant pathways associated with the DEGs. There were 23 pathways at day 10, 10 at day 21 and 12 at day 40 of post-wounding that were significantly enriched in DEGs ($P<0.05$; Figs. 6-8). These KEGG pathways were associated with 'metabolism', 'environmental information processing', 'organismal systems', and 'human diseases'. At Stage 1, 'infectious diseases' were markedly enriched in DEGs (Fig. 6B); at Stage 2, 'amino acid metabolism' and 'lipid metabolism' were also enriched in DEGs (Fig. 7B); at Stage 3, 'cancers' and 'signal transduction' were significantly enriched in DEGs (Fig. 8B). The present data suggested that the functions of DEGs were varied during different stages.

Identification of signaling pathways. Through further analysis of the differences in signaling pathways in different stages, it was identified that among several differently expressed signaling pathways from the proliferative stage to the tissue remodeling stage, the expressions of Wnt2B, Wnt-5, secreted frizzled-related protein 4 (SFRP4) and dishevelled binding antagonist of β catenin 2 (DACT2) genes, related to the Wnt/β-catenin signaling pathway, were significantly different. The expression of Wnt 2B and Wnt-5 in the hypertrophic scar

Table I. Mapping results.

Sample	Useful reads	Map events count	Mapped reads	Mapped, %	Multiple mapped reads	Multiple mapped, %	Uniquely mapped reads	Uniquely mapped, %
1HS	38,267,666	31,678,684	28,051,392	73.30	1,592,461	5.68	26,458,931	94.32
1C	38,590,244	31,198,001	28,285,531	73.30	1,366,137	4.83	26,919,394	95.17
2HS	39,054,466	30,707,726	28,477,397	72.92	1,063,918	3.74	27,413,479	96.26
2C	35,269,558	28,070,605	26,132,568	74.09	990,225	3.79	25,142,343	96.21
3HS	35,543,910	28,868,026	26,660,182	75.01	1,004,164	3.77	25,656,018	96.23
3C	35,078,178	28,628,227	26,151,005	74.55	1,096,865	4.19	25,054,140	95.81

HS, hypertrophic scarring; C, control.

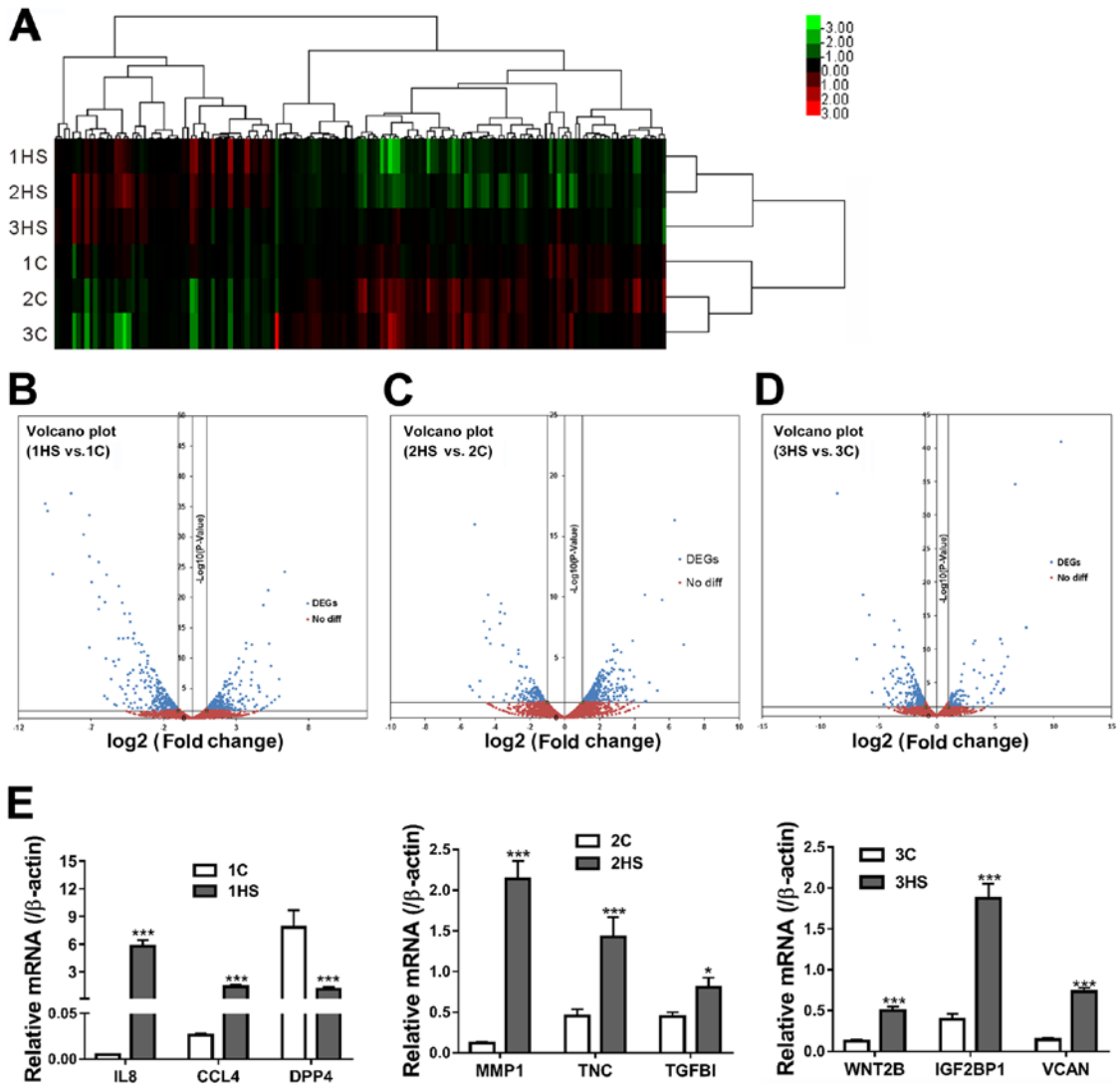

Figure 4. Identification of DEGs. (A) A heat map shows hierarchical clustering of gene expression in different samples. (B-D) Volcano plots depict fold changes (log2, x-axis) in individual gene expression in HS tissues (1HS, 2HS and 3HS) vs. corresponding C samples (1C, 2C and 3C), and statistical significance [-log10 (P-value), y-axis]. (E) Validation of RNA-sequencing data by reverse transcription-quantitative PCR. *P<0.05, ***P<0.001 vs. respective C. DEGs, differentially expressed genes; HS, hypertrophic scarring; C, control; IL8, interleukin-8; CCL4, C-C motif chemokine ligand 4; DPP4, dipeptidyl peptidase 4; MMP-1, matrix metalloproteinase-1; TNC, tenascin C; TGFβ1, transforming growth factor β-1; WNT2B, Wnt family member 2B; IGF2BP1, insulin-like growth factor 2 mRNA-binding protein 1; VCAN, versican; diff, difference.

was several times higher than that in the remodeling scar. However, the expression of SFRP4, an antagonist of the Wnt signaling pathway, was significantly higher in the remodeling scar than that in HS (Data S1 and S2). In contrast to scars

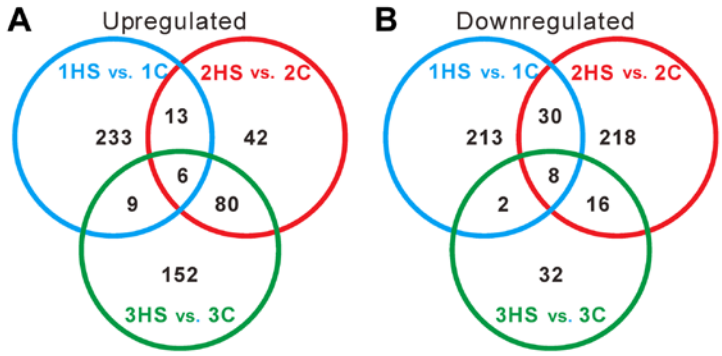

Figure 5. Venn diagrams of DEGs. (A) Overlap of upregulated DEGs. (B) Overlap of downregulated DEGs. DEGs, differentially expressed genes; HS, hypertrophic scarring; C, control.

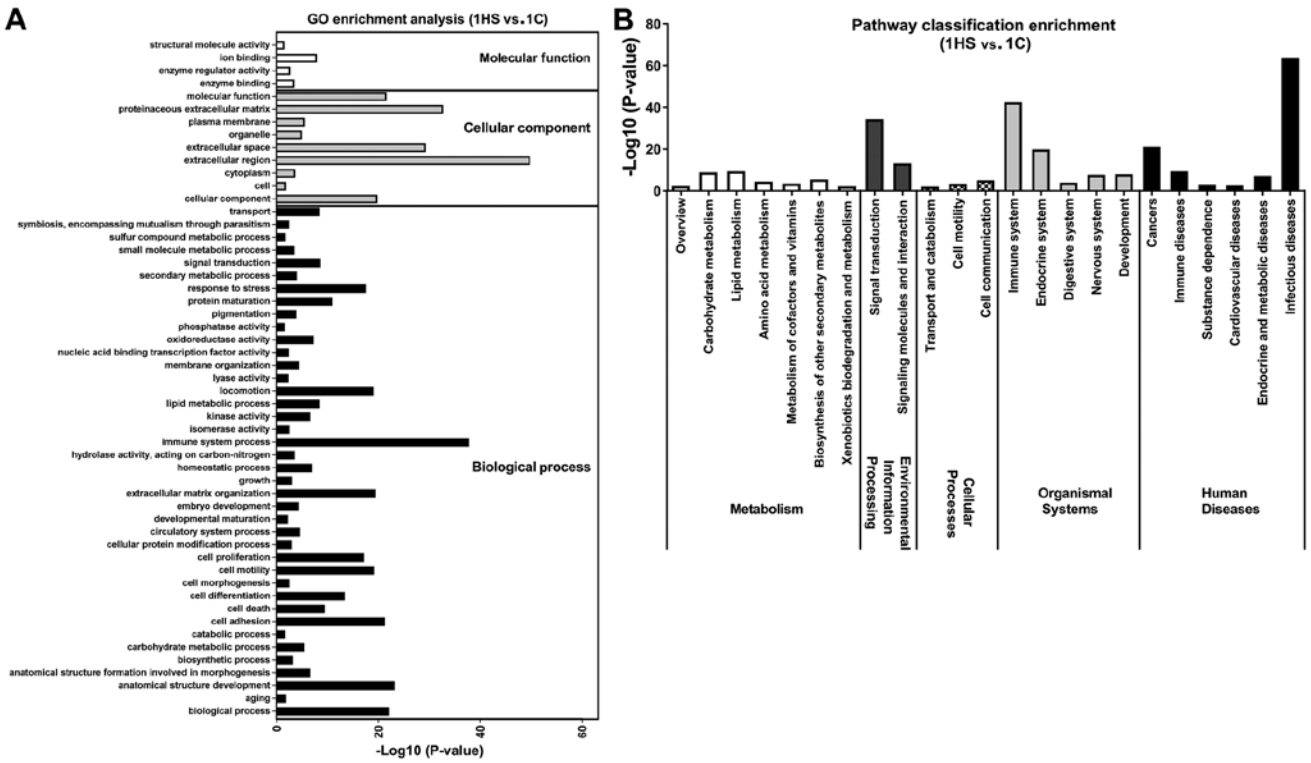

Figure 6. GO and KEGG pathways enrichment of differentially expressed genes between 1HS and 1C. (A) GO term enrichment analysis. A total of 22 terms show significant differences (P<0.05) in three main categories (biological process, cellular component and molecular function). (B) KEGG pathway classification enrichment analysis (P<0.05). GO, Gene Ontology; KEGG, Kyoto Encyclopedia of Genes and Genomes; HS, hypertrophic scarring; C, control.

Table II. Differential expression of Wnt/β-catenin signaling pathway-related genes in different stages of scarring.

	Proliferation stage/tissue remodeling stage			
Gene	Control samples	P-value	HS	P-value
Wnt2B	3.371	0.032	-	-
Wnt-5	4.348	0.000	2.941	0.014
SFRP4	0.0267	0.000	0.140	0.013
DACT2	0.071	0.000	-	-

SFRP4, secreted frizzled-related protein 4; DACT2, dishevelled-binding antagonist of β-catenin 2; -, undetected differential expression; HS, hypertrophic scarring.

in the HS region, the differences in the expression were more significant in the normal receding surrounding scars (Table II).

Discussion

The roles of various fibrotic and anti-fibrotic molecules in the formation of HS have been studied (5,9,11). In the present study, an animal model of HS using rabbit ears was established and was then analyzed using RNA-Seq for both HS and C samples at different stages. To the best of the authors' knowledge, this is the first investigation on the gene expression profiling of HS using the RNA-Seq technique. A total of 17,386 unigenes were functionally annotated to the eggNOG database. 'Signal transduction mechanisms' was the largest category, which indicated that the unigenes were mainly involved in regulating signal

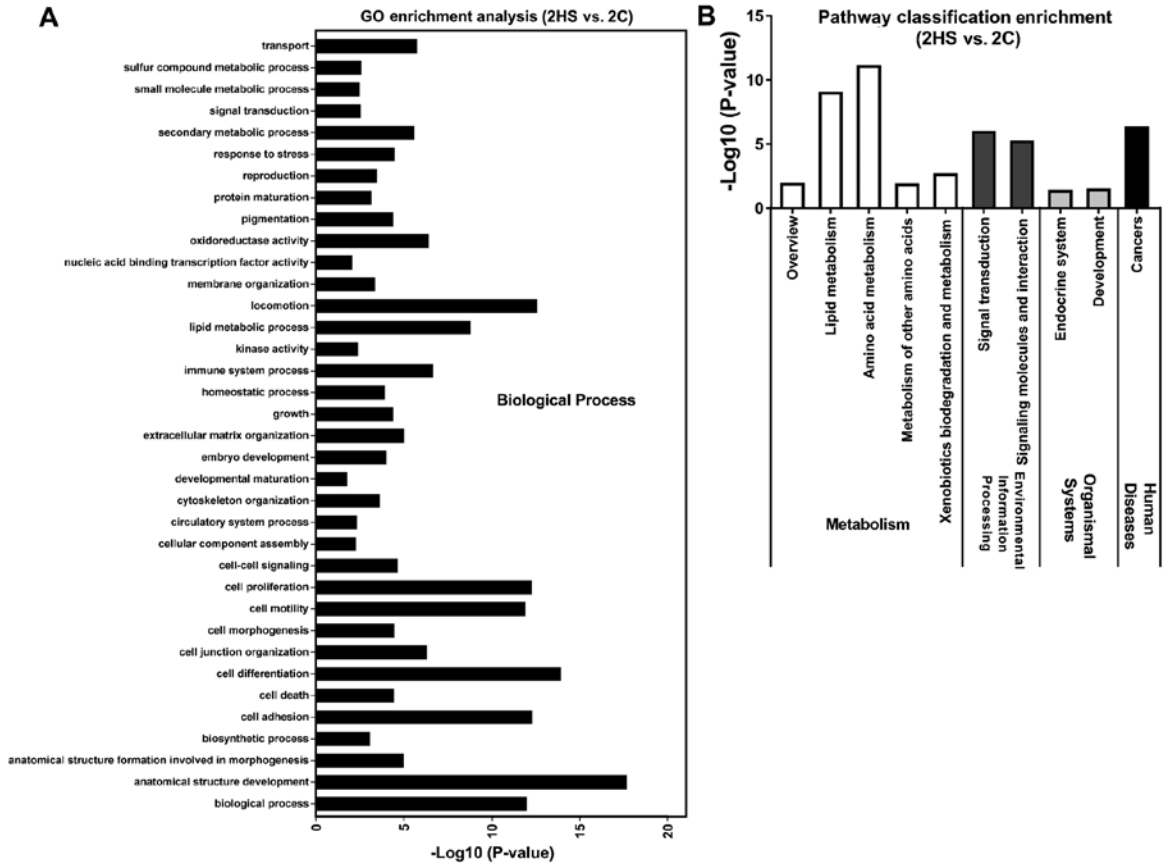

Figure 7. GO and KEGG pathways enrichment of differentially expressed genes between 2HS and 2C. (A) GO term enrichment analysis (P<0.05). (B) KEGG pathway classification enrichment analysis (P<0.05). GO, Gene Ontology; KEGG, Kyoto Encyclopedia of Genes and Genomes; HS, hypertrophic scarring; C, control.

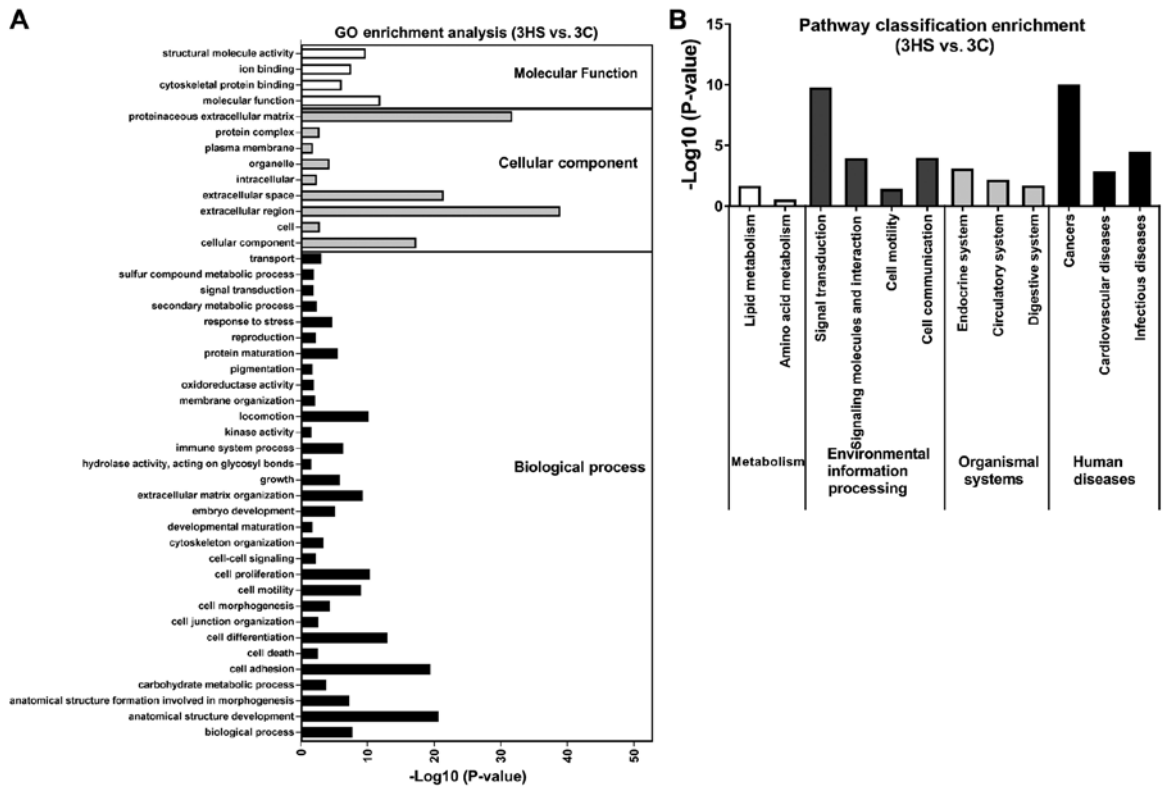

Figure 8. GO and KEGG pathways enrichment of differentially expressed genes between 3HS and 3C. (A) GO terms enrichment analysis (P<0.05). (B) KEGG pathway classification enrichment analysis (P<0.05). GO, Gene Ontology; KEGG, Kyoto Encyclopedia of Genes and Genomes; HS, hypertrophic scarring; C, control.

transduction post-wounding. A total of 514, 413 and 305 DEGs were identified at days 10, 21 and 40 post-wounding, respectively, compared with the corresponding C group (1C, 2C and 3C). RT-qPCR assays validated the RNA-Seq results. Several DEGs have been linked to the pathogenesis of HS, such as TGFβ1 (4), connective tissue growth factor (4), CXCR3 (8), CXCR4 (7), IL8, DPP4 (19), toll like receptor 4 (9), TNC (8), VCAN (20), MMP1 and MMP9 (10,11). Numerous genes, such as CCL4, WNT2B, IGF2BP1, fatty acid binding-protein 9 and cadherin 20 have not previously been studied in HS, to the best of the authors' knowledge. The data suggested the robustness of RNA-Seq in quantifying and annotating transcriptomes. The present results suggested that the inflammatory reaction and immune response were the main reactions in the wound healing process, which was consistent with the human wound healing process, and also demonstrated the reliability of the results of the transcriptional analysis.

The hierarchical clusters and Venn diagrams indicated that the identified DEGs were varied among different stages. Furthermore, the GO function enrichment and KEGG pathway enrichment analyses on these DEGs provided information for understanding the molecular mechanisms of HS pathogenesis. A total of three stages, including inflammation, proliferation and tissue remodeling, were defined during wound healing and scarring (1). At Stage 1, DEGs were enriched in GO terms and KEGG pathways involved in 'immune system process', 'proteinaceous extracellular matrix', which is consistent with that the initial stage of healing, that includes cell migration and inflammation (21). Cell proliferation, angiogenesis and matrix synthesis occurred, following the initial stage of healing (1). As hypothesized at Stage 2, DEGs were enriched in GO terms and KEGG pathways involved in 'anatomical structure development', 'cell differentiation', 'cell adhesion', 'cell proliferation', 'cell motility', 'amino acid metabolism' and 'lipid metabolism'. In the tissue remodeling phase of wound healing, inflammatory cells and mesenchymal cells underwent apoptosis with a reduction in vascularity and collagen synthesis. It was identified that DEGs were enriched in the functions associated with 'cancers', 'proteinaceous extracellular matrix', and 'signal transduction' at Stage 3. Moreover, other GO terms and KEGG pathways were enriched at each stage, which provided comprehensive expression and functional profiles during the formation of HS.

To identify more effective treatment methods for patients with HS, the differences in the molecular signaling pathway between HS and remodeled scars were compared to explore the breakthrough point to promote the regression of HS. The differences in the Wnt/β-catenin signaling pathway related to gene expression were highly significant in scar transition from the proliferative stage to the tissue remodeling stage. The expressions of Wnt-2 and Wnt-5 in HS were several times higher than that in tissue remodeling scars, while the expression of SFRP4 in hypertrophic scars was notably lower than that in tissue remodeling scars, and the difference was more significant in the C samples than in HS. As an antagonist of Wnt ligands, SFRP4 can inhibit the classical Wnt signaling pathway (22). SFRP4 was first found to be upregulated in increased apoptosis in C3H/10T½ cells (23). Several tumors, such as endometrial, cervical, ovarian, prostate, bladder, colorectal, mesothelioma, pancreatic, renal and esophageal are characterized by aberrant promoter hypermethylation, which causes variations in the expression levels of SFRP4 when compared to normal cells (24). Upregulated SFRP4 alleviated myocardial fibrosis induced by ischemic injury and improved myocardial function (25), and inhibited angiogenesis *in vivo* and *in vitro* (26). These previous results suggested that the Wnt signaling pathway may play a pivotal role in the transition from HS to the tissue remodeling stage, and regulation of the Wnt signaling pathway may promote the regression of HS.

In summary, gene expression profiling in HS and C samples demonstrated significant differences in transcriptional levels among different stages of HS. Novel DEGs were also identified during the formation of HS. Furthermore, GO terms and KEGG pathways identified differences in biological pathways and processes among different stages. The Wnt signaling pathway was found to play an important role in the regression of HS. The present study provided insight for the comprehensive understanding of the mechanisms of HS formation and might be helpful in the development of potential therapeutic treatments for individuals with HS following injury.

Acknowledgements

Not applicable.

Funding

The present study was supported by The Shanghai Natural Science Foundation (grant no. 15ZR1413500).

Availability of data and materials

The datasets used and/or analyzed during the current study are available from the corresponding author on reasonable request.

Authors' contributions

JZ and MS performed the experiments. MS drafted the manuscript. JZ revised the manuscript. YW and HB analyzed the data. CX and JZ designed the study. All authors read and approved the final manuscript.

Ethics approval and consent to participate

All animal experiments were approved by The Institutional Animal Care and Use of The Second Military Medical University.

Patient consent for publication

Not applicable.

Competing interests

The authors declare that they have no competing interests.

References

1. Zhu Z, Ding J, sky Shankowsky HA and Tredget EE: The molecular mechanism of hypertrophic scar. J Cell Commun Signal 7: 239-252, 2013.
2. Aarabi S, Longaker MT and Gurtner GC: Hypertrophic scar formation following burns and trauma: New approaches to treatment. PLoS Med 4: e234, 2007.

3. Tyack Z, Simons M, Spinks A and Wasiak J: A systematic review of the quality of burn scar rating scales for clinical and research use. Burns 38: 6-18, 2012.
4. Penn JW, Grobbelaar AO and Rolfe KJ: The role of the TGF-β family in wound healing, burns and scarring: A review. Int J Burns Trauma 2: 18-28, 2012.
5. Niessen FB, Schalkwijk J, Vos H and Timens W: Hypertrophic scar formation is associated with an increased number of epidermal Langerhans cells. J Pathol 202: 121-129, 2004.
6. Morris DE, Wu L, Zhao LL, Bolton L, Roth SI, Ladin DA and Mustoe TA: Acute and chronic animal models for excessive dermal scarring: Quantitative studies. Plast Reconstr Surg 100: 674-681, 1997.
7. Ding J, Hori K, Zhang R, Marcoux Y, Honardoust D, Shankowsky HA and Tredget EE: Stromal cell-derived factor 1 (SDF-1) and its receptor CXCR4 in the formation of postburn hypertrophic scar (HTS). Wound Repair Regen 19: 568-578, 2011.
8. Yates CC, Krishna P, Whaley D, Bodnar R, Turner T and Wells A: Lack of CXC chemokine receptor 3 signaling leads to hypertrophic and hypercellular scarring. Am J Pathol 176: 1743-1755, 2010.
9. Wang J, Hori K, Ding J, Huang Y, Kwan P, Ladak A and Tredget EE: Toll-like receptors expressed by dermal fibroblasts contribute to hypertrophic scarring. J Cell Physiol 226: 1265-1273, 2011.
10. Eto H, Suga H, Aoi N, Kato H, Doi K, Kuno S, Tabata Y and Yoshimura K: Therapeutic potential of fibroblast growth factor-2 for hypertrophic scars: Upregulation of MMP-1 and HGF expression. Lab Invest 92: 214-223, 2012.
11. Ulrich D, Noah EM, von Heimburg D and Pallua N: TIMP-1, MMP-2, MMP-9, and PIIINP as serum markers for skin fibrosis in patients following severe burn trauma. Plast Reconstr Surg 111: 1423-1431, 2003.
12. Zhu S, Qing T, Zheng Y, Jin L and Shi L: Advances in single-cell RNA sequencing and its applications in cancer research. Oncotarget 8: 53763-53779, 2017.
13. Liu YJ, Zhang F, Liu HD and Sun X: The application of next-generation sequencing techniques in studying transcriptional regulation in embryonic stem cells. Yi Chuan 39: 717-725, 2017.
14. Sarig O and Sprecher E: The molecular revolution in cutaneous biology: Era of next-generation sequencing. J Invest Dermatol 137: e79-e82, 2017.
15. Saulis AS, Mogford JH and Mustoe TA: Effect of Mederma on hypertrophic scarring in the rabbit ear model. Plast Reconstr Surg 110: 177-183, 2002.
16. Syed F, Ahmadi E, Iqbal SA, Singh S, McGrouther DA and Bayat A: Fibroblasts from the growing margin of keloid scars produce higher levels of collagen I and III compared with intralesional and extralesional sites: Clinical implications for lesional site-directed therapy. Br J Dermatol 164: 83-96, 2011.
17. Livak KJ and Schmittgen TD: Analysis of relative gene expression data using real-time quantitative PCR and the 2(-Delta Delta C(T)) method. Methods 25: 402-408, 2001.
18. Jensen LJ, Julien P, Kuhn M, von Mering C, Muller J, Doerks T and Bork P: eggNOG: Automated construction and annotation of orthologous groups of genes. Nucleic Acids Res 36: D250-D254, 2008.
19. Walmsley GG, Rinkevich Y and Hu MS: Identification and targeted inhibition of a fibroblast lineage responsible for skin scarring and cancer stroma. J Am Coll Surg 219: S84-S85, 2014.
20. Scott PG, Dodd CM, Tredget EE, Ghahary A and Rahemtulla F: Immunohistochemical localization of the proteoglycans decorin, biglycan and versican and transforming growth factor-beta in human post-burn hypertrophic and mature scars. Histopathology 26: 423-431, 1995.
21. Aarabi S, Bhatt KA, Shi Y, Paterno J, Chang EI, Loh SA, Holmes JW, Longaker MT, Yee H and Gurtner GC: Mechanical load initiates hypertrophic scar formation through decreased cellular apoptosis. FASEB J 21: 3250-3261, 2007.
22. Kawano Y and Kypta R: Secreted antagonists of the Wnt signaling pathway. J Cell Sci 116: 2627-2634, 2003.
23. Melkonyan HS, Chang WC, Shapiro JP, Mahadevappa M, Fitzpatrick PA, Kiefer MC, Tomei LD and Umansky SR: SARPs: A family of secreted apoptosis-related proteins. Proc Natl Acad Sci USA 94: 13636-13641, 1997.
24. Maganga R, Giles N, Adcroft K, Unni A, Keeney D, Wood F, Fear M and Dharmarajan A: Secreted frizzled related protein-4 (sFRP4) promotes epidermal differentiation and apoptosis. Biochem Biophys Res Commun 377: 606-611, 2008.
25. Matsushima K, Suyama T, Takenaka C, Nishishita N, Ikeda K, Ikada Y, Sawa Y, Jakt LM, Mori H and Kawamata S: Secreted frizzled related protein 4 reduces fibrosis scar size and ameliorates cardiac function after ischemic injury. Tissue Eng Part A 16: 3329-3341, 2010.
26. Muley A, Majumder S, Kolluru GK, Parkinson S, Viola H, Hool L, Arfuso F, Ganss R, Dharmarajan A and Chatterjee S: Secreted frizzled-related protein 4: An angiogenesis inhibitor. Am J Pathol 176: 1505-1516, 2010.